Temperature-Dependent Raman Scattering of Silicon Nanowires

Zixue Su,[†] Jian Sha,*[,†] Guowei Pan,[†] Jianxun Liu,[†] Deren Yang,[†] Calum Dickinson,[‡] and Wuzong Zhou*[,‡]

Department of Physics, State Key Lab of Silicon Materials, Zhejiang University, Hangzhou 310027, People's Republic of China, and School of Chemistry, University of St. Andrews, St. Andrews, Fife KY16 9ST, United Kingdom

Received: October 13, 2005; In Final Form: December 2, 2005

Silicon nanowires with narrowly distributed diameters of 20−30 nm have been fabricated by chemical vapor deposition on an anodized aluminum oxide (AAO) substrate. The first-order and second-order Raman scatterings of the silicon nanowires have been studied in a temperature range from 123 to 633 K. Both of the first-order and second-order Raman peaks were found to shift and broaden with increasing temperature. The experimental results were analyzed by combining the phonon confinement effect, anharmonic phonon processes and lattice stress effect. It was found that the intensities of the first-order and second-order Raman bands have different dependences on temperature. The value of relative intensities $I(2TA)_{int}/I(2TO)_{int}$ for silicon nanowires was found to be larger than that of bulk silicon, and increase with rising measurement temperature. We ascribe this phenomenon to the participation of phonons with a large wave vector value of Raman scattering caused by both the phonon confinement effect and the temperature effect.

I. Introduction

Nanoscale semiconductors have triggered tremendous technological and scientific interest due to the unique electronic and optical properties, and potential industrial applications. Silicon nanowires in particular are attractive due to their interesting physical properties of conductivity, light emission, and field emission and due to their suitability to be used as building blocks for various electronic nanodevices in the microelectric industry.[1−3]

The properties of silicon nanowires depend on their microstructures and dimensions. Raman spectroscopy is one of the nondestructive techniques used to study the microstructures of solids via their vibrational properties. For example, examination of line shapes of Raman spectra may give useful information of crystallinity, amorphicity, and dimensions of nanoscale silicon. Raman scattering of crystalline silicon in various forms, such as bulk, nanoparticles, and nanowires, has been investigated extensively in the last 40 years.[4−6] The temperature effect on the first-order Raman scattering in silicon materials has also been studied thoroughly and a peak shift was observed in bulk and nanocrystalline silicon specimens with increasing temperature.[7−9] Raman spectroscopy of amorphous and nanocrystalline α-Si:H films was also investigated.[10,11] It was found that the second-order acoustic bands 2LA (longitudinal acoustic) and 2TA (transverse acoustic) do not seem to be influenced by confinement effects and are similar to those in the bulk. The second-order optic bands are broadened and shifted in comparison to those in the bulk. It has been known that, in addition to the first-order Raman scattering, higher order Raman scattering may also give important information of vibrational properties of nanocrystalline silicon and, therefore, attracted much attention from scientists in the past few years.[12]

Restricted to the Raman selections rule, only the transverse optical (TO) phonon mode is Raman active during the first-order scattering process for silicon nanowires. The investigation of the temperature dependence of high-order Raman spectra, by considering the participation of other phonons in the scattering process, will help us to acquire information of vibrational properties and phonon related interaction of silicon nanowires which cannot be obtained merely from the first-order Raman spectra. Moreover, silicon is a semiconductor that has an indirect band gap with low light emission efficiency. So far, porous silicon and silicon nanocrystallites were found to have efficient photoluminescence covering almost the whole range from infrared to ultraviolet region. During the electron transition process for the materials with an indirect band gap, the participation of single phonon or multiphonon is inevitable. The study of electron−phonon and photon−phonon processes in the temperature-dependent Raman spectra is therefore useful for further investigation of the light emission of silicon nanowires. However, to the best of our knowledge, there is no report on the temperature effect on the high-order Raman spectra in silicon nanowires.

In the present work, we studied the temperature effect on the first-order and second-order Raman scatterings of silicon nanowires within the temperature range from 123 to 633 K. It was found that both of the first-order and second-order Raman peaks downshifted and broadened from those of bulk silicon. This is due to the phonon confinement in the nanowires. Additionally, the increasing temperature added further downshift and broadening of the peaks. The relative intensities of the second-order bands and the first-order bands also depend on the measurement temperature. The value of relative intensities $I(2TA)_{int}/I(2TO)_{int}$ for silicon nanowires is larger than that for bulk silicon, and increases with the temperature.

II. Experimental Section

Anodized aluminum oxide (AAO) substrates and chemical vapor deposition (CVD) technique were used for preparing the array-ordered silicon nanowires.[13] A pure Al plate (1 mm thick, 99.99%) was annealed at 500 °C for 2 h in a vacuum, then

* Address correspondence to these authors. E-mail: phyjsha@zju.edu.cn or wzhou@st-andrews.ac.uk.
[†] Zhejiang University.
[‡] University of St. Andrews.

10.1021/jp055869o CCC: $33.50
Published on Web 12/31/2005

washed with acetone. The plate was anodized at 16 °C in oxalic acid solution at a constant voltage of 42 V for 3 h, forming an anodic oxide layer. The structure of the top part of this layer was disordered, which was then removed in a mixed solution of phosphoric acid and chromic acid. After this removal, the Al plate was anodized again for 10 h under the same conditions as the first anodizing step. A bilayer plate was produced with porous alumina on one side and aluminum on the other. The latter was then dissolved in a saturated $CuCl_2$ solution, leaving an alumina plate with about a 10 μm thickness, and this was further treated in phosphoric acid at 30 °C for 90 min. An AAO substrate with pores sub-100 nm in diameter was eventually prepared.[14]

Gold was deposited on one side of the AAO substrate by using the magnetron sputtering method.[15] The Au-deposited alumina substrate was placed into a tube furnace and the pressure in the furnace chamber was pumped down to 20 Pa. The substrate was heated to the pre-set point of 500 °C before the mixed gases of argon, hydrogen, and silane with a ratio of 10: 20:15 were allowed to flow into the chamber. The temperature and pressure were kept constant, 500 °C and 1400 Pa, respectively, during the deposition. After 6 h of deposition, the furnace was cooled to room temperature and the AAO substrate with newly formed silicon nanowires was removed from the furnace and stored in a desiccator.

Initial characterization of the specimens was performed with high resolution transmission electron microscopy (HRTEM). TEM images, showing directly the morphologies and sizes of the nanowires, and HRTEM images, showing atomic structures and surface coating, were obtained from a Phillip CM2000 electron microscope operating at 200 KV.[16] The purity of the Si nanowires was examined by using energy-dispersive X-ray spectroscopy (EDX). For the HRTEM studies, the alumina substrate was dissolved in ethanol, and one drop of Si nanowire suspension was deposited on a copper grid precoated with a holey carbon film.

The micro-Raman backscattered spectra were recorded on a Raman spectrometer (Nicolet Thermo) using an Ar-ion laser with a wavelength of 532 nm. The spectra resolution was about 1 cm^{-1}. The spot size of the incident light was approximately 1 mm^2 on the sample. Raman experiments on the sample were performed at different temperatures varying between 123 and 633 K with a laser power of 30 mW. To clarify the possible effect caused by laser induced local heating, the Raman spectra of the silicon nanowires were illuminated by different laser powers from 9 to 30 mW.

III. Results and Discussion

Templated by the holes in the alumina substrate, the produced silicon nanowires have narrowly distributed diameters of about 20−30 nm (Figure 1). Figure 1b shows a typical HRTEM image from a thin nanowire. It was found that all the nanowires have an amorphous coating layer, which has also been commonly observed by other groups.[2,3] The chemical composition of the coating layer is mainly silicon. However, the presence of a small percentage of oxygen was also detected by EDX. The diameter of the crystalline silicon core is about half of the whole diameter of the nanowire. Amorphous surface coating layers are often found in other nanomaterials produced by the CVD method. In a previous HRTEM investigation of Mg_2SiO_4 fishbone-like fractal nanostructures, we found that the amorphous surface layer did not result from decomposition of the crystalline nanowires, but from deposition of the source materials.[17] We believe the amorphous layer of SiO_x on the silicon nanowires plays a similar

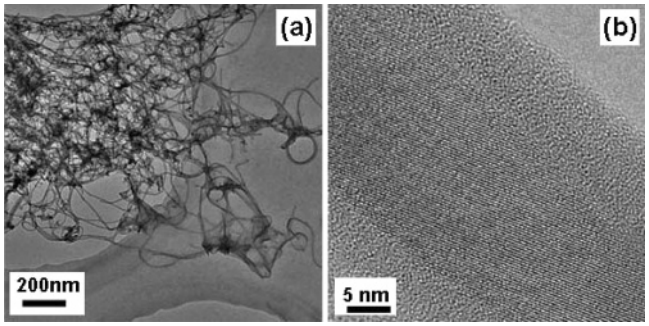

Figure 1. (a) TEM image showing the produced silicon nanowires. (b) HRTEM image of a typical silicon nanowire, showing an amorphous coating layer of about 10 nm thickness.

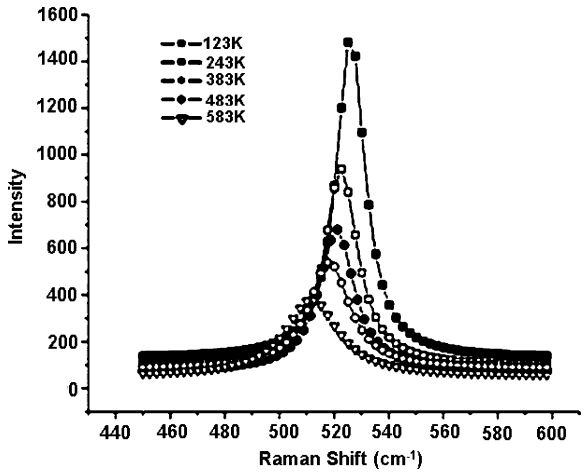

Figure 2. The Gauss fit of the first-order Raman lines of the silicon nanowires with different measurement temperatures.

role and the full discussion will be reported separately (C. Dickinson et al., manuscript in preparation). According to a previous report by Fukata et al., a shift of Raman peak caused by an amorphous layer 15 nm thick in silicon nanowires with a total diameter of 45 nm was ignorable. When the thickness of the amorphous layer increased to 20 nm and the diameter of the silicon core decreased to 6 nm, the corresponding shift resulting from the amorphous layer was no more than 0.8 cm^{-1}.[18] Therefore, the contribution of the amorphous layer to the shift of Raman peaks in the present work could be ignored.

Figure 2 shows the gradual modification of the first-order Raman spectra of the silicon nanowires with temperature varying from 123 to 583 K. As the temperature rises, the intensity of the TO phonon mode decreases, the full width of half-maximum (fwhm) broadens, and the peak position shifts toward lower frequency.

During the course of our investigation of the laser effect on Raman spectra, we found that a strong laser power may increase the local temperature in the nanoscale specimens of silicon and affect the Raman spectra. This effect is very much insignificant in bulk silicon. The possible reason is that the thermal conductivity of silicon nanowires is poorer than that of the bulk silicon due to the lower dimensions. Thereby, in the investigation of temperature-dependent Raman spectra of silicon nanowires, the laser power must be maintained at a relatively low value to avoid serious local heating. To examine the local heating effect by the laser irradiation, Raman scattering was performed with different powers. As the laser power was increased from 9 to 30 mW, the intensity of the TO phonon mode increased. However, no obvious Raman shift for the TO mode was found, and the change of the asymmetry of the Raman line was also

very small (Figure 3). Consequently, under the current experimental conditions, the power density on the sample was rather low and the local heating on the sample during the laser beam irradiation was not significant. This observation is different from the previous report by Piscanec et al. in which they found that serious local heating on the sample even with a power less than 30 mW had a significant effect on the Raman spectra of silicon nanowires.[6] The possible reason for this difference is that the silicon nanowires produced in the present work had a much thicker amorphous coating, about 10 nm instead of 2 to 3 nm in the samples made by Piscanec et al.[6] The laser had to penetrate through a thick amorphous layer before reaching the crystalline core. The actual power received by the crystalline silicon nanowires therefore would be reduced substantially. Consequently, the results in Figure 3 enable us to conclude that the local heating effect induced by laser, in the present work, can be ignored.

It has been established that, due to the relaxation of the fundamental wave vector $q \sim 0$ Raman selections rule, phonons away from the Brillouin-zone center are allowed to participate in the scattering, which leads to downshift and asymmetric broadening of the Raman peaks of silicon. Otherwise, heating the sample will cause symmetric broadening and downshift of Raman peaks of silicon due to the anharmonic phonon processes. Therefore, we combine the effects of phonon confinement and anharmonic phonon processes to interpret the Raman spectra of silicon nanowires. Following the work by Campbell et al.[19] and Richter et al.[20] and considering the anharmonic phonon processes, the intensity of a Raman peak is given by

$$I(\omega) = \int_0^1 \frac{\exp(-q^2L^2/4a^2)}{[\omega - \omega(q,T)]^2 + [(\Gamma(T)/2]^2}\, \mathrm{d}^3q \qquad (1)$$

where

$$\omega(q,T) = \omega(q) + \Delta(T) + \Delta(L)$$

$$\omega(q) = [A + B\cos(q\pi/2)]^{1/2}$$

$$\Delta(T) = C\left[1 + \frac{2}{e^{\hbar\omega/2k_BT} - 1}\right] + D\left[1 + \frac{3}{e^{\hbar\omega/3k_BT} - 1} + \frac{3}{(e^{\hbar\omega/3k_BT} - 1)^2}\right]$$

$$\Gamma(T) = \Gamma_0 + \Gamma_1 + E\left[1 + \frac{2}{e^{\hbar\omega/2k_BT} - 1}\right] + F\left[1 + \frac{3}{e^{\hbar\omega/3k_BT} - 1} + \frac{3}{(e^{\hbar\omega/3k_BT} - 1)^2}\right]$$

In the above equations, $\omega(q)$ is the phonon dispersion curve in bulk silicon. $A = 1.714 \times 10^5$ cm^{-2}, and $B = 1.000 \times 10^5$ cm^{-2}. q is expressed in units of $2\pi/a$, where a is the lattice constant of silicon. ΔT is the frequency shift caused by anharmonic phonon processes. L corresponds to the average diameter of silicon nanowires. $\Delta(L)$ is the frequency shift due to the phonon confinement effect and the lattice stress effect. $\Gamma(T)$ is the mode line width and C, D, E, and F are anharmonic constants (cm^{-1}): $C = -3.996$, $D = -0.235$, $E = 1.683$, $F = 0.136$.[21] Γ_0 is the fwhm of the reference bulk silicon and Γ_1 is the line width broadened by phonon confinement and the lattice stress effect.

When $\Delta(L) = 2.8$ cm^{-1}, the calculated and the experimentally observed temperature dependence of the Raman shift of the active TO mode have good agreement as shown in Figure 4. There is also good agreement between the calculated and the experimental values of the line width with $\Gamma_1 = 10.5$ cm^{-1} (Figure 5). Consequently, in comparison with bulk crystalline silicon, the nanowires have a downshift of 2.8 cm^{-1}, a broadening of 10.5 cm^{-1}, and a certain degree of asymmetry. Furnace heating gives further downshift and symmetric broadening.

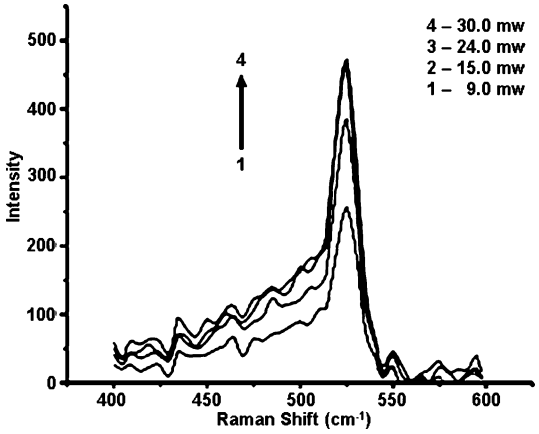

Figure 3. The first-order Raman lines of silicon nanowires with varying laser power.

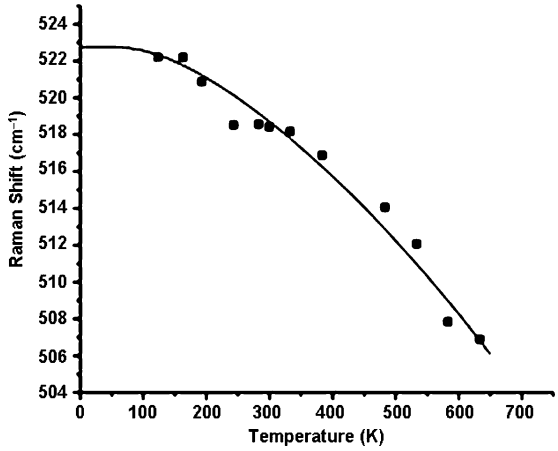

Figure 4. Temperature dependence of frequency shift for the Raman active TO mode in the silicon nanowires. The curve gives the theoretical fit with the anharmonic phonon processes. The squares represent the experimental results.

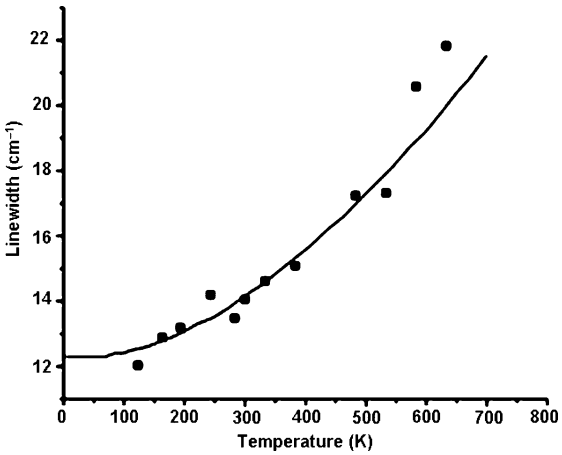

Figure 5. Variation of fwhm for the first-order optic mode in the silicon nanowires with measurement temperature. The curve gives the theoretical fit with anharmonic phonon processes. The squares represent the experimental results.

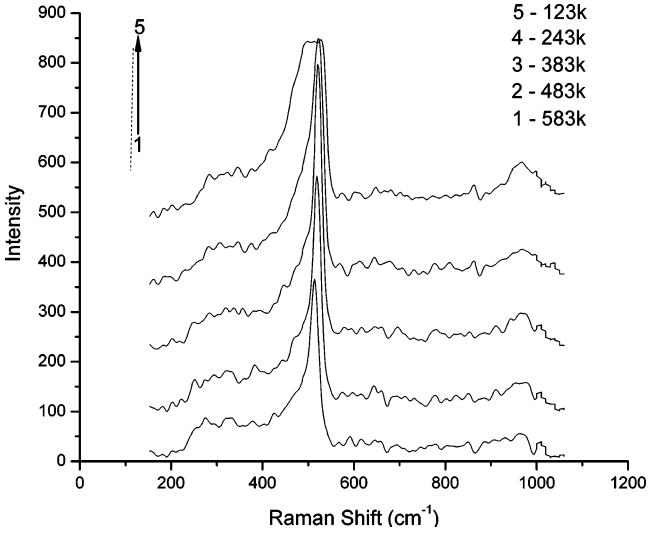

Figure 6. Variation of the second-order Raman lines of silicon nanowires with measurement temperatures. The dash line with positive slope helps to discern the downshift of frequency.

As mentioned above, the average diameter of the nanowires is very small and all the nanowires are wrapped by a thick amorphous layer of SiO_x. These properties may cause lattice stress in the nanowires.[12] According to the XRD results, the cubic unit cell parameter (a) of the silicon nanowires is 0.5448 nm, which is 0.313% larger than its bulk counterpart with $a_0 =$ 0.5431 nm. This indicates a slight lattice expansion of the structure in silicon nanowires. The corresponding small lattice stress results in a Raman shift determined by the following equation:[22]

$$\Delta\omega = -n\upsilon\omega_0\frac{a - a_0}{a_0} \qquad (2)$$

where n is the dimensionality of the materials ($n = 1$), υ is the Gruneisen constant with a value of 0.98, and ω_0 is the Raman peak position of bulk silicon (520 cm^{-1}). a and a_0 are the cubic unit cell parameters of silicon nanowires and bulk silicon, respectively. On the basis of eq 2 the Raman shift caused by the lattice expansion is about 1.6 cm^{-1}. Consequently, in the 2.8 cm^{-1} Raman shift of silicon nanowires from the standard value of bulk silicon, there is about a 1.2 cm^{-1} frequency shift that can be attributed to the phonon confinement effect and the lattice stress gives a Raman shift of about 1.6 cm^{-1}. Taking into account the discrepancy of line width between the nanowires and the bulks, the lattice stress effect should give about 10 cm^{-1} broadening of the fwhm, and the broadening of the fwhm induced by the phonon confinement effect is less than 1 cm^{-1}.

In Figure 6, we can see that both the second-order acoustic bands and optic bands downshift and broaden with rising temperature. This is due to their fundamental phonon modes downshifting and their fwhm broadening significantly with the change of measurement temperature. The higher order bands of silicon nanowires downshift and broaden consequently.

According to Mishra and Jain's research on α-Si:H films,[10] the acoustic bands were found not to be influenced by the confinement effect and the ratio of the integrated intensities $I(2TO)_{int}/I(TO)_{int}$ varies with the nanocrystal size, but does not depend on the heating power densities, i.e., temperature. However, in the present work, we found that the intensities of the first-order band drops when temperature was increased and the relative integrated intensities of the second-order bands and

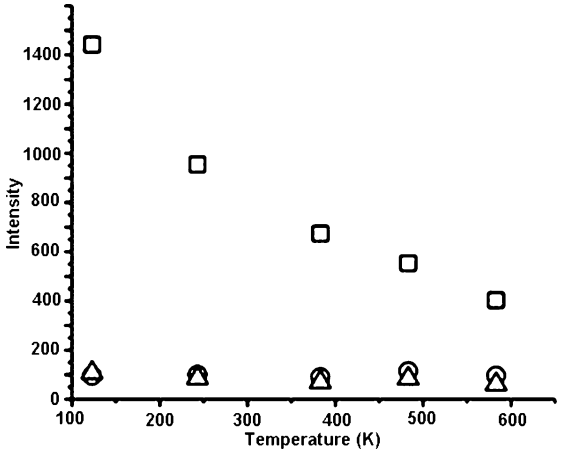

Figure 7. Variation of integrated intensity of the phonon modes with measurement temperatures. The squares correspond to the intensities of the TO mode, the circles correspond to the 2TA mode, and the triangles correspond to the 2TO mode.

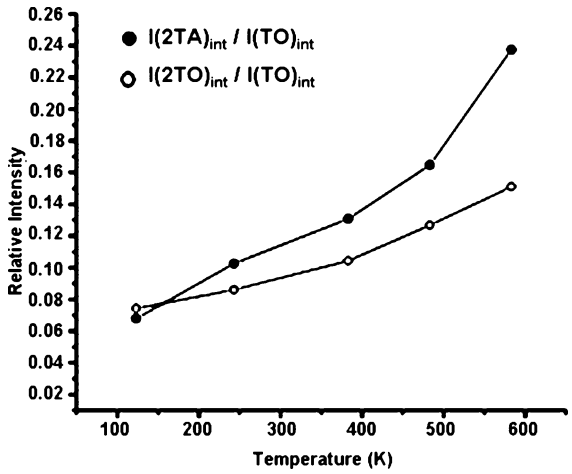

Figure 8. Variation of integrated intensity ratios of the second-order bands and the first-order band with measurement temperature. The solid circles correspond to 2TA/TO, the open circles correspond to 2TO/TO.

the first-order optic mode clearly increased with the increase of the measurement temperature (see Figures 7 and 8).

We ascribe these phenomena to different temperature dependences of the scattering section between the first-order bands and the second-order bands. When the measurement temperature rises, the state density of phonons, which have a higher energy, will increase. This will induce a reduction of the intensity of Stokes scattering and an increase of the intensity of anti-Stokes scattering. On the other hand, the temperature-dependent hot activated phonon population of the vibrational state is given by the Bose−Einstein distribution function, viz., $n(\omega,T) = [\exp(\hbar\omega/k_BT) - 1]^{-1}$. For one-phonon and two-phonon processes, relations between the Raman scattering section and temperature can be written as $\sigma \propto n(\omega,T)$ and $\sigma \propto \{n(\omega,T)\}\{n(\omega',T)\}$, respectively. The scattering sections of the second-order bands and the first-order bands are decided by both factors described above. That is why the intensity of the first-order band drops as the temperature rises as shown in Figure 2, and the relative integrated intensities $I(2TA)_{int}/I(TO)_{int}$ and $I(2TO)_{int}/I(TO)_{int}$ increase as temperature rises. On the other hand, the intensities of the first-order Raman lines of silicon nanowires increase with the laser power as shown in Figure 3. This result implies again that the increase of local temperature resulting from the laser irradiation is not significant, otherwise the intensities of the first-

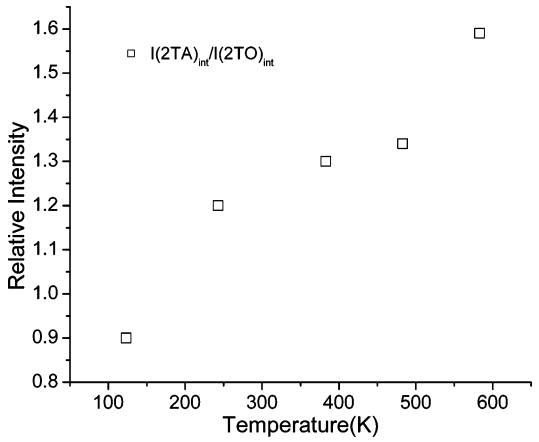

Figure 9. Variation of the relative intensity $I(2TA)_{int}/I(2TO)_{int}$ with measurement temperature.

order bands would decrease with the laser power. The reason for the enhanced intensities of the first-order Raman lines, shown in Figure 3, is the higher quantity of the incident photons associated with the increased laser power, resulting in more phonons to participate in the scattering.

In Figure 9, we can see that the relative intensity $I(2TA)_{int}/I(2TO)_{int}$ increases obviously with rising temperature. The value of $I(2TA)_{int}/I(2TO)_{int}$ increases from 0.9 at 123 K to 1.59 at 583 K. The acoustic phonon mode seems to have higher scattering efficiency than the optic mode with the rising of the measurement temperature. In another comparison, the value of $I(2TA)_{int}/I(2TO)_{int}$ is 0.54 for bulk silicon but 1.08 for the silicon nanowires at 300 K. To understand these observations we take the following consideration.

The Hamilton quantum of the interaction between energy band electrons and acoustic phonons is given by:

$$H_{ep} = -i\sum_{k}\sum_{q,s}\left(\frac{N\hbar}{2M\omega_{qs}}\right)^{1/2} V_{q+k_n}\{e_{qs}(q+k_n)\} \times (a_{qs} + a^{+}_{-qs})C^{+}_{k'}C_k$$

$$k' = k + q + k_n$$

k', k, and q are all reduced wave vectors, and they are in the first Brillouin zone. When $k + q$ is in the first Brillouin zone, $k_n = 0$, $k' = k + q$, the total wave vector remains a constant. With the method of long wave approximation, e_{qs} has roots parallel to or perpendicular to the wave vectors q, representing the LA and TA phonon, respectively. Obviously, in the case of $k + q$ in the first Brillouin zone, $e_{qT}q = 0$, $e_{qs}(q + k_n) = e_{qL}\cdot q$, only the LA phonons participate in the interaction with the energy band electrons. However, when q has a larger value, $k + q$ is out of the first Brillouin zone. For $k_n \neq 0$, $k' = k + q + k_n$, $e_{qT}q = 0$, $e_{qT}k_n \neq 0$, both the LA phonons and the TA phonons interact with the energy band electrons. Since a higher temperature allows more scattering processes with q of a large value, the interaction between the acoustic phonons and the energy band electrons becomes more significant. During the Raman scattering, we propose that a photon−electron−phonon process occurs. The incident light interacts with the energy band electrons first, and then the phonons participate in the interaction, as discussed above, with the energy band electrons. Therefore, more acoustic phonons will participate in the Raman scattering process at a higher temperature when q is large. In the case of optic phonons, the transverse electromagnetic wave field induced by the incident light interacts with the optic phonons, whether the vector $k + q$ is in the first Brillouin zone or not. On the basis of the discussion above, we can understand that the value of $I(2TA)_{int}/I(2TO)_{int}$ should indeed increase with the measurement temperature.

For the larger value of $I(2TA)_{int}/I(2TO)_{int}$ from silicon nanowires in comparison with bulk silicon, a similar consideration could be taken as follows. Due to the phonon confinement effect, the fundamental $q \sim 0$ Raman selection rule relaxes, phonons with larger values of q are allowed to participate in the scattering in silicon nanowires. This will cause an increase of the value of $I(2TA)_{int}/I(2TO)_{int}$. In the relaxation of the Raman selection rule due to the Heisenberg uncertainty principle, the smaller dimension of the nanowires allows phonons with a larger value of q to participate in the scattering since the phonon uncertainty goes roughly as $\Delta q \sim 1/L$, where L is the diameter of the nanowires. We can therefore make a prediction that the value of $I(2TA)_{int}/I(2TO)_{int}$ may increase when the diameter of silicon nanowires is reduced.

IV. Conclusion

Silicon nanowires were prepared by the CVD process on an AAO substrate. The temperature-dependent Raman spectra of silicon nanowires were analyzed by combining the phonon confinement effect, anharmonic phonon processes, and the lattice stress effect. Both of the first-order and second-order Raman peaks were found to shift and broaden with increasing temperature. The ratios of the integrated intensities $I(2TO)_{int}/I(TO)_{int}$ and $I(2TA)_{int}/I(TO)_{int}$ increased with the increase of the measurement temperature due to the different temperature dependences of the scattering sections of the first-order and the second-order bands. The interactions of the incident light with acoustic phonons and optic phonons were influenced by temperature differently. The value of relative intensities $I(2TA)_{int}/I(2TO)_{int}$ for silicon nanowires was found to be larger than that for bulk silicon, and increases with rising temperature. The participation of phonons with a large value of q in the Raman scattering caused by phonon confinement and temperature effect was introduced as an explanation. The present work will be useful for further investigation of the electron−phonon and photon−phonon interactions, and of benefit to the future study of the light emission properties of nanostructured silicon.

Acknowledgment. This work was supported by National Natural Science Foundation of China (No. 20240430654, 50272057), Zhejiang Provincial 151 project, and the Center for Nanoscience and Nanotechnology of Zhejiang University. W.Z. thanks EPSRC for the studentship to C.D.

References and Notes

(1) Cui, Y.; Lieber, C. M. *Science* **2001**, *291*, 851.
(2) Shi, W. S.; Peng, H. Y.; Zheng, Y. F.; Wang, N.; Shang, N. G.; Pan, Z. W.; Lee, C. S.; Lee, S. T. *Adv. Mater.* **2000**, *12*, 1343.
(3) Morales, A. M.; Lieber, C. M. *Science* **1998**, *279*, 208.
(4) Russell, J. P. *Appl. Phys. Lett.* **1965**, *6*, 223.
(5) Mishra, P.; Jain, K. P. *Phys. Rev. B* **2000**, *62*, 14790.
(6) Piscanec, S.; Cantoro, M.; Ferrari, A. C.; Zapien, J. A.; Lifshitz, Y.; Lee, S. T.; Hofmann, S.; Robertson, J. *Phys. Rev. B* **2003**, *68*, 241312.
(7) Hart, T. R.; Aggarwal, R. L.; Lax, B. *Phys. Rev. B* **1970**, *1*, 638.
(8) Tsu, R.; Hernandez, J. G. *Appl. Phys. Lett.* **1982**, *41*, 1016.
(9) Balkanski, M.; Wallis, R. F.; Haro, E. *Phys Rev. B* **1983**, *28*, 1928.
(10) Mishra, P.; Jain, K. P. *Phys. Rev. B* **2001**, *64*, 073304.
(11) Bhusari, D. M.; Kumbhar, A. S.; Kshirsagar, S. T. *Phys. Rev. B* **1993**, *47*, 6460.
(12) Wang, R. P.; Zhou, G. W.; Liu, Y. L.; Pan, S. H.; Zhang, H. Z.; Yu, D. P.; Zhang, Z. *Phys. Rev. B* **2000**, *61*, 16827.

(13) Qi, J. F.; White, J. M.; Belcher, A. M.; Masumoto, Y. *Chem. Phys. Lett.* **2003**, *372*, 763.
(14) Zhang, H.; Ma, X. Y.; Xu, J.; Niu, J. J.; Sha, J.; Yang, D. R. *J. Cryst. Growth* **2002**, *246*, 108.
(15) Liu, J. X.; Niu, J. J.; Yang, D. R.; Yan, M.; Sha, J. *Phys. E* (*Amsterdam, Neth.*) **2004**, *23*, 221.
(16) Zhou, W.; Thomas, J. M. *Curr. Opin. Solid State Mater. Sci.* **2001**, *5*, 75.
(17) Xie, S.; Zhou, W.; Zhu, Y. Q. *J. Phys. Chem. B* **2004**, *108*, 11561.
(18) Fukata, N.; Oshima, T.; Murakami, K.; Kizuka, T.; Tsurui, T.; Ito, S. *Appl. Phys. Lett.* **2005**, *86*, 213112.
(19) Campell, I. H.; Fauchet, P. M. *Solid State Commun.* **1986**, *58*, 739.
(20) Richter, H.; Wang, Z. P.; Ley, L. *Solid State Commun.* **1981**, *39*, 625.
(21) Konstantinovic, M. J.; Bersier, S.; Wang, X.; Hayne, M.; Lievens, P.; Silverans, R. E.; Moshchalkov, V. V. *Phys. Rev. B* **2002**, *66*, 161311.
(22) Bruesch, P. *Phonons: Theory and Experiments I—Lattice Dynamics and Models of Interatomic Forces*; Springer: Berlin, Germany, 1982.